DTU Library

Decisive parameters for moisture safe internal insulation of masonry − Long time monitoring in inhabited dwellings

Pagoni, Panagiota; B. Møller, Eva; H. Peuhkuri, Ruut

Published in:
Energy and Buildings

Link to article, DOI:
10.1016/j.enbuild.2024.114180

Publication date:
2024

Document Version
Publisher's PDF, also known as Version of record

Energy & Buildings 312 (2024) 114180

Contents lists available at ScienceDirect

Energy & Buildings

journal homepage: www.elsevier.com/locate/enb

Decisive parameters for moisture safe internal insulation of masonry – Long time monitoring in inhabited dwellings

Panagiota Pagoni [a,*], Eva B. Møller [a], Ruut H. Peuhkuri [b]

[a] Technical University of Denmark, Brovej 118, 2800, Kgs. Lyngby, Denmark
[b] Aalborg University, A. C. Meyers Vænge 15, 2450, Copenhagen, Denmark

ARTICLE INFO

Keywords:
Internal insulation
Residential building
Mold growth
Hygrothermal performance
Retrofitting
Building façade
Monitoring
Hydrophobization

ABSTRACT

Most buildings in Europe were constructed between 1850 and 1960, a period in which energy efficiency was not considered much. However, many of these structures have architecturally valuable facades that should be preserved, making internal thermal insulation the only practical solution. Therefore, internal insulation has grown in popularity despite the potential risk of moisture-related problems behind the insulation and on the external surface of the original wall. To ensure the structure's durability and the residents' wellbeing, insulating solutions must undergo real-life testing to demonstrate their effectiveness and moisture safety.

The present paper is a compilation of case studies performed over the last decade in Denmark, it compares across four case studies of residential buildings. The apartments were insulated internally with either diffusion-tight or diffusion open and capillary active insulation systems. In some of the cases, internal insulation was applied in combination with hydrophobization of the existing facade. Temperature and relative humidity were measured in the indoor climate, at the intersection between insulation and masonry, and in some cases also at the wooden beam ends or the spandrels. Additionally, the risk of mold growth was calculated. The current study focuses on the wall's hygrothermal performance in relation to the thickness of the masonry and insulation, the wall's orientation, the indoor moisture excess, the effects of hydrophobization and the role of indoor climate. The results indicate that – while internal insulation of masonry more or less result in expected energy savings – areas with thin masonry or very thick insulation give an increased risk for mold growth. In addition, high indoor moisture excess in combination with diffusion open insulation system increases the risk for mold growth, while the other parameters played a less decisive role.

1. Introduction

In recent years, internal insulation has undergone a product and method development to solve some of the technical construction problems with the insulation method. Internal insulation has high potential as an energy improvement for the part of the general housing mass that was built as a time-typical brick buildings up to the 1960s [1,2]. For the insulation method to be more widespread, it must be robust and proven suitable. Internal post-insulation has been much debated, as there has been examples of homes where the insulation has resulted in mold growth on the inside of the outer wall [2,3]. In these homes, indoor climate problems have arisen that have affected the health of residents [4]. Other homes with interior post-insulation have apparently not had similar problems with the indoor climate.

This study aims to evaluate in a real-life setting and examine the hygrothermal effects of multiple types of internal insulation systems, thickness of masonry and insulation material, and hydrophobization, on the hygrothermal conditions at the interface of internal insulation and masonry, and in certain cases, at the wooden beam ends. Additionally, the effect was evaluated by measuring the energy saving and the risk of indoor climate problems using a mold growth model.

1.1. Motivation

The current study is motivated by the combination of the climate action plans of European and Danish authorities and increasing awareness to decrease space heating consumption while preserving the architectural features of traditional masonry, and achieving a more comfortable and healthy interior environment [5]. Internal insulation is believed to be a way to reconcile these goals. Thus, the current study's

* Corresponding author.
E-mail addresses: papag@dtu.dk (P. Pagoni), ebmo@dtu.dk (E. B. Møller), rup@build.aau.dk (R. H. Peuhkuri).

https://doi.org/10.1016/j.enbuild.2024.114180
Received 20 October 2023; Received in revised form 4 April 2024; Accepted 12 April 2024
Available online 14 April 2024

objective is to show how to reduce energy consumption in a moisture-safe way. Additionally, this study will help to learn more about construction technology and the robustness of the insulation method connected to user behavior. Based on the robustness of the insulation method and construction in combination with the user behavior, the study can also pinpoint which parameters are the most important to be aware of to reduce the risk of moisture induced indoor climate problems.

1.2. State of the art

41 % of the multi-story Danish buildings were constructed between 1850 and 1960 [4]. The built environment is responsible for 30–40 % of all $C0_2$ emissions [6]. Like the ones in the current study, buildings of this type are often constructed with solid brick masonry walls and wooden beam ends embedded in the wall [3]. These structures lack thermal insulation, which increases the potential for energy savings. Nevertheless, only internal adjustments are feasible due to historical, aesthetic, and architectural reasons [3,5,7]. However, thermal insulation from inside poses a risk as thermal bridges cannot be avoided and the original wall is left exposed and cold [8,9]. Also, the use of the insulation material may result in decreased vapor diffusion inwards. In addition, the insulation's steep temperature gradient increases the danger of mold growth and moisture problems at the insulation's interface with the cold external wall. Risks are influenced by the temperature both inside and outside, the moisture level, and the vapor permeability of the internal insulation system [4]. Therefore, it is necessary to find and test sustainable methods and solutions for wall refurbishment that only provide limited risk for wood rot or mold growth [3,7]. The external surface of the wall might also be hydrophobized as an extra technique to reduce the external moisture load, as the treatment stops capillary suction. Hydrophobization is an almost invisible and irreversible treatment [10]. There is a variety of previous studies, such as [6,8,11–15], which focus on the robustness and moisture safety of internal insulation in older buildings as well and use relevant methodologies to examine the properties and risks of the different internal insulation systems.

1.2.1. Internal insulation

Internal post-insulation causes a large temperature drop in the original wall in areas with cold climate, which results in even lower temperatures on the external side of the wall [1,8,16]. This leads to reduced drying capability and perhaps increased moisture content in the wall when combined with covering the internal surface of the wall with a material. As a result, there is a possibility of moisture-related issues like frost damage at the exterior surface, rot in the wooden beam ends, high relative humidity, or even interstitial condensation at the interface of internal insulation and the original wall, where, as a result, mold may appear [2,17–19].

In recent years, focus on interior insulation of historic structures has been increasing. Harrestrup et al. [20] observed the impact of deliberate thermal bridges around the wooden beams in a case of interior insulation with 40 mm Aerowolle (composite of aerogel and mineral wool) on a historical brick building. There was a decreased risk of mold growth when a 200 mm uninsulated gap was left in the beam ends, although this was shown to be highly dependent on the orientation and thickness of the original wall. A 19th-century building with solid brick walls, utilized as kindergarten, with external render, hydrophilic mineral wool insulation board on the inside, and no vapor barrier was the focus of the 4-year study by Toman et al. [21]. Although, no vapor retarder was installed, acceptable hygrothermal conditions were observed and there was no risk of interstitial condensation. Two cases of internal insulation made of calcium silicate and lightweight aerated concrete on a solid brick wall were studied by Walker et al. [22]. The results showed no critical moisture conditions as the structure was protected from external moisture loads with an exterior curtain wall. Unfortunately, measurements only lasted for six months. On the other hand, throughout the course of a 9 month investigation, Klõšeiko et al. [23] tested four internal insulation materials and found high relative humidity. The materials were monitored for interstitial condensation and mold growth risk. Calcium silicate had the maximum heat conductivity of the tested materials, and it had the best performance in terms of moisture safety.

1.2.2. Diffusion open and tight insulation systems

Both diffusion open and tight insulation systems are examined in the current study. An insulation material's microstructure with a closed pore structure, possibly combined with a foil as a vapor barrier on the insulation material's warm side, makes a diffusion-tight system. Two conditions must be fulfilled for the traditional diffusion tight internal insulation to prevent indoor climate problems: 1) to prevent water from penetrating from the outside; the exterior surface of the external wall must be watertight. Thus, the masonry must be intact, 2) the vapor barrier must be tightly fitted and placed correctly; no more than a third of the insulation when measured from the warm side to ensure that relative humidity stays below critical values [16].

On the other hand, careful installation is also necessary for the diffusion open and capillary-active materials without a vapor barrier to perform properly. For capillary active and diffusion open insulation materials, the moisture that has been absorbed at the interface can be redistributed and allowed to evaporate inwards when the conditions are right [2]. All capillary active systems must be tightly fitted to the existing wall to prevent air pockets behind the insulation. Otherwise, moisture cannot be sucked from the areas without physical contact, and favorable conditions for mold growth may occur. Internal post-insulation can be problematic even when these conditions are met; this especially applies to thermal bridges, which appear when floors or partitioning walls meet the external walls. Due to internal post-insulation, the temperature is further decreased and the relative humidity rises in the areas of the thermal bridges [3]. However, thermal bridges may be also used to reduce the risk; if there is a gap in the insulation near the floor, the area will still be warm, and the moisture risk will not be the same as before. Because there are many prerequisites that must be fulfilled, internal post-insulation is considered a challenging solution.

1.2.3. Moisture sources and protection

The amount of moisture in the wall relies on both the external and internal moisture loads, as well as the initial built-in moisture. Three main forms of external moisture loads might have an impact on the performance of the external walls of masonry: water vapor from the humid outdoor air, liquid water from the wind driven rain – WDR [2] and liquid water from the rising damp. The inhabitants' daily humidity production while living in the apartments causes the internal moisture load. This moisture load is normally managed by a vapor tight layer as described in previous section. In external walls made of porous materials like brick and mortar, as in these projects, WDR may particularly be crucial [2,8,17]. The current study examines and compares the south orientation for WDR (WDR with south-west orientation is dominant in Denmark) with the north orientation. The quantity of rain and wind, along with the material's qualities and any potential flaws like broken joints, bricks, or render that allow air pressure to drive water through the wall, determine how easy WDR can penetrate porous building materials [18]. Additionally, summer condensation can occur when solar radiation warms up the external side of the wall, causing the moisture to penetrate deeper into the wall [24]. Other moisture sources, like rising damp, will be relevant for some structures, especially for basements and walls in ground floor.

Older masonry may benefit from external rain protection like hydrophobization since it can prevent or at least obstruct the penetration of precipitation by effectively blocking the capillary suction without effecting the vapor diffusion of the wall, as shown in [8] and [17]. However, experimental results on the combination of hydrophobization with internal insulation in solid masonry walls also show in certain studies [25,26] that the effect of hydrophobization not always is positive. Both diffusion open and tight insulation systems are subject to this problem.

1.2.4. Risk of mold growth

Avoiding excess moisture is essential for healthy and durable buildings. Mold growth is one of the consequences and the first signs of too high moisture loads in indoor air and building constructions. Biological growth like mold growth is unwanted in indoor air and constructions in connection to indoor environment, as it can compromise the indoor air quality and the health of the occupants, e.g. by causing respiratory system issues [27]. However, there might be places where some mold growth would be acceptable, e.g., embedded beam ends if there is no transfer of air from the moldy area to the indoor air [28]. Jensen [29] examined a few common VOCs (Volatile Organic Compounds) produced by fungi. The water vapor permeability of the insulation has been found to be correlated with the ability of the VOCs to move to the interior environment [29]. Favorable conditions for mold growth are: High humidity levels (typically > 75 % RH) and temperatures within a certain range (20–30 °C) in a necessary period of time, together with nutrition availability like organics compounds and/or dust [30,31]. When applying internal insulation, there is a risk of that favorable conditions for mold growth are created in the interface between the original wall and the insulation. Removing all the wallpaper and glue lowers the likelihood of mold growth since it can provide nutrition for fungi, if it is present [27]. In the case of a vapor tight insulation system mold risk applies in the case where the insulation or

Table 1
Facade with indication of insulated walls, and sensor placement on floor plan.

Cases	Building facade	Floor plan of apartment
M		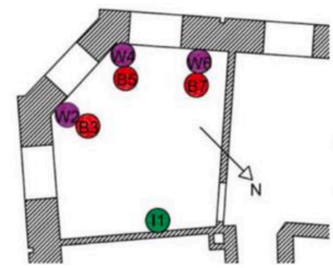 Red (B3, B5 and B7): wooden beam ends Purple (W2, W4 and W6): intersection Green (I1): internal climate
D		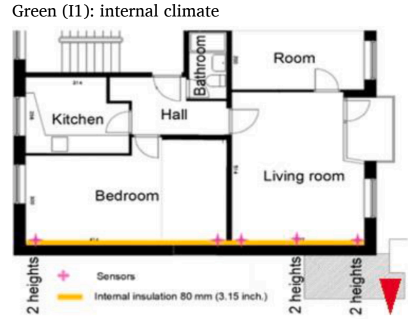 Pink stars: interface sensors Yellow lines: insulation
B		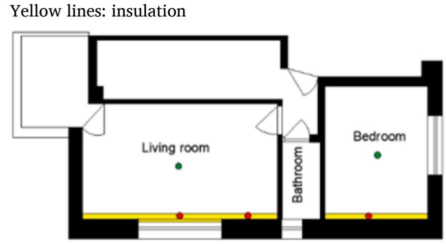 Green: indoor climate sensors Red: interface sensors Yellow lines: insulation
F	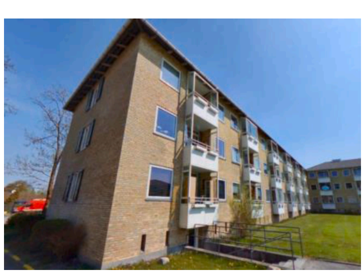	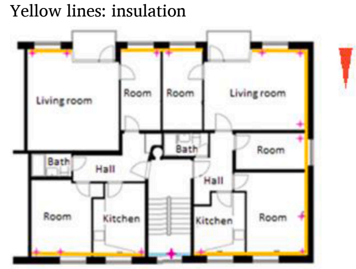 Pink stars: interface sensors Yellow lines: insulation Blue line: staircase insulation

vapor barrier is compromised and air can be transferred to the interface. In addition, inadequate heating during the winter can further lower the temperatures and increase the relative humidity.

2. Method and materials

2.1. Description of the cases

In the section below the methods and materials are presented. In all cases, the masonry was inspected for damage before internal post-insulation was applied and, if damage was found, small repairs took place. The information and details about the cases are gathered in Table 1, Table 2, and Table 3. Information about the four cases are also found in [16,24,32].

For all cases, the detail of the wall construction and the placement of the sensors is shown in Fig. 1.

2.2. Construction and materials

In all cases, the walls were cleaned of organic material, such as internal rendering, wallpaper, and paint, and imperfections were straightened with new plaster before the internal insulation was installed. The external surface of the brick wall was without rendering. In all cases (except case M), the insulation system was placed completely adhered to the original wall, and consisted of the following layers: original wall, glue mortar, insulation, and finishing layer (with reinforcing mesh and diffusion open paint). In case M, there was also gypsum board as part of the insulation system, and diffusion tight paint. Additionally, the humidity class for every case was determined according to the international standard EN ISO 13788 [33]. The humidity class based on measurements of indoor and outdoor temperature and relative humidity. According to the moisture excess [g/m^3] and temperature in each apartment/case there is a corresponding humidity class. In the next sections, the humidity classes for each of the cases are presented, along with further information and details.

In two cases (M and B), a silane-based, water-based cream with a 40 % concentration was used as hydrophobization agent. Before the hydrophobization, the renovation process involved replacing any bricks that were broken or damaged and repointing the joints. Following the manufacturer's instructions, the hydrophobization product was applied in one coat using a roll brush after letting the walls cure for two weeks.

2.2.1. Case M

The location of this case is in the center of Copenhagen, Denmark. It is a multi-story residential masonry structure constructed in 1877 in the typical Danish construction style, with wooden beams separating the floors [16]. The 5th floor's external walls were insulated during the winter of 2014. Additionally, a 20 cm gap above the floor was used to intentionally create a thermal bridge (see Fig. 2). Fig. 2 depicts the wall's construction in detail, including the placement of the sensors (for sensor description, see Table 5). The measurements were made between the winter of 2014 and the spring of 2018. Six years after the insulation, in the fall of 2020, the building's whole façade underwent renovation, including repointing, before being hydrophobized [32]. After that, the measurements resumed.

Table 3
Information of the original wall and hydrophobization for each case.

Case	Original wall	Hydrophobization
M	1 ½ brick (350 mm) solid masonry, spandrel 1 brick (228 mm)	No + Yes
B	1 ½ brick (360 mm) solid masonry, spandrel 1 brick (228 mm)	No + Yes
D	1 ½ brick (360 mm) masonry with multi-hole brick on external side and lightweight clinker concrete on the internal side (half and half).	No
F	1 ½ brick (360 mm) masonry with multi-hole brick on external side and lightweight clinker concrete on the external side (half and half).	No

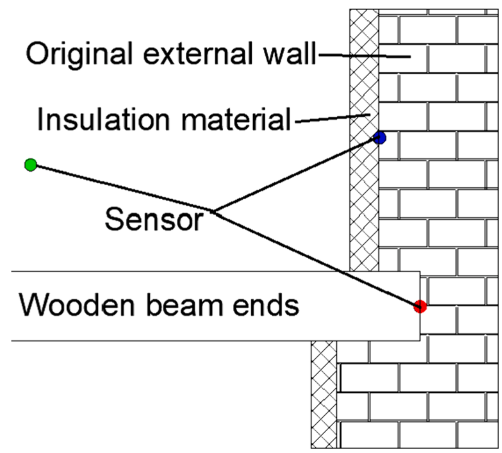

Fig. 1. Wall construction and sensor placement. Blue: wall interface, Green: internal, Red: wooden beam ends (only in case M). (For interpretation of the references to colour in this figure legend, the reader is referred to the web version of this article.)

2.2.2. Case B

The location of this case is in Copenhagen's northwest. This case involved four identical multi-story residential buildings constructed in 1940. Internal insulation was installed in one gable wall of each test apartment, four gables in total (two north-facing and two south-facing). As a reference, one uninsulated apartment was chosen. One gable wall for each direction (one north and one south), underwent hydrophobization [32]. Two sensors (one in every room) were used to

Table 2
Information on insulation materials.

Case	Insulation Material	Thickness (mm)	λ-value (W/mK)	U-value (W/m^{2}K)	Type	μ-value (−)	Orientation
M	Phenolic Foam (with gypsum board and alufoil)	60 (20 at spandrels)	0,02	0,27	Dif. tight	35	SW
B	Autoclaved lightweight AAC	100 (220 at spandrels)	0,042	0,33	Dif. open + cap. active	2	N + S
D	Autoclaved lightweight AAC	80	0,042	0,35	Dif. open + cap. active	2	N
F	Polyurethane foam with calcium silicate	80:gable wall 50:façade 15:window reveal	0,033	0,29:gable 0,41:facade 0,72:window reveal	Dif. tight	27	N + S + W
	Autoclaved calcium silicate	50:staircase	0,05		Dif. open + cap. active	15	N

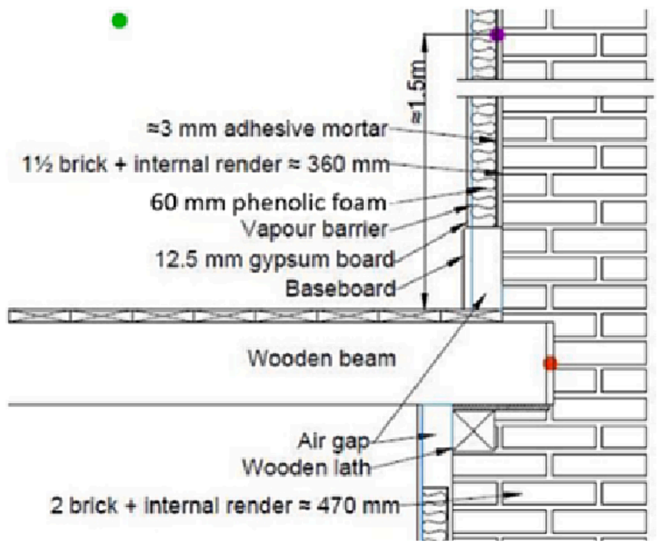

Fig. 2. Construction detail with sensor placement. Red (B3, B5 and B7): wooden beam ends. Purple (W2, W4 and W6): intersection. Green (I1): internal climate [16]. (For interpretation of the references to colour in this figure legend, the reader is referred to the web version of this article.)

measure the indoor hygrothermal conditions, and three sensors (one at the spandrel and two in the center of the external wall) were used to measure the conditions at the interface between the original wall and the insulation material. The measurements began in the fall of 2018 and were finished in the summer of 2020. Information on the five case apartments are shown in Table 4.

2.2.3. Case D

In this case, a three-story residential structure in Copenhagen's southwest is examined. It is a part of a larger building complex that includes numerous other buildings erected similarly between 1952 and 1962. The walls are made of a combination of yellow multi-hole bricks and clinker concrete (Fig. 3), and the floor partitioning of concrete slaps. The external walls of three north-facing gable apartments, one on top of another, were insulated during summer of 2015. Fig. 3 depicts the top view of the structure with a small part of the gable covered by the next building. Each apartment included eight sensors, all of them installed at the interface between the original wall and the insulation. Table 1 shows where the sensors were installed. They were placed about in the center of the height of the wall and in three areas supplemented by sensors mounted near the floor. Hygrothermal measurements began in winter of 2015 and continued until summer of 2023 when most of the sensors stopped working. Energy use for heating was registered from April 2016 to March 2017, but excluding June-September, which is outside the heating season. Indoor climate measurements (temperature and relative humidity) were measured before and after interior insulation installation; from September 2014 to August 2015 and from March 2016 to June 2017.

Three apartments in a similar building were used as reference apartments. The reference apartments were also on top of each other

Table 4
Information about the apartments of case B, including the time of the installation.

Apartment	Floor	Orientation	Hydrophobization	Internal insulation system
A1	3rd	N	Yes (mid Sept-18)	Yes (start/mid Oct-18)
A2	2nd	S	Yes (mid Oct-18)	Yes (start Oct-18)
A3	4th	N	No	Yes (mid Sept-18)
A4	5th	S	No	Yes (start Nov-18)
Reference	2nd	S	No	No

Table 5
Information of sensors.

Case	Sensor type	Accuracy of sensors	Logging interval	Area of placement	Measuring condition
M	Rotronic HygroClip2 (HC2)	±1 K and ± 0.8 % RH (up to 90 % RH)	1 min.	Interfaces, Beam ends, Indoors	T, RH
B	Rotronic HL-RC-B with HC2A-S	±0.1 °C and ± 0.8 % RH	1 hr.	Interfaces	T, RH
	HOBO data logger (U12-012)	±0.35 °C and ± 2.5 % RH	1 hr.	Indoors	T, RH
D	Hygro-I T/RF	±0.3 °C and ± 1.8 % RH	30 min.	Interfaces	T, RH
	Lascar EL USB 2+	±0.45 °C and ± 2.05 % RH	30 min.	Indoors, Outdoors	T, RH
F	Tramex Hygro-I ®	±0.3 °C and ± 1.8 % RH (10 % to 90 %)	30 min.	Interfaces Indoors	T, RH

with a north-facing gable. No energy-saving measures were installed in these apartments; they were only used for measuring indoor climate (temperature and relative humidity) from 2016 to 2017 and energy consumption for the same heating season.

2.2.4. Case F

This case is a part of the same complex as Case D, the original components are therefore the same. In summer 2015, post-insulation was established [24]. From the beginning of 2016 until the start of 2022, the hygrothermal conditions at the interface between the insulation and the existing wall have been measured. In a three-story building, all six apartments around one staircase were used for the measurements; on each floor, one apartment was "in the middle of the building" i.e. only having two facades as outer walls, and one apartment also had a gable (see Table 1). The facades (facing north and south) of all six apartments, and the gables (facing west) of the three 'end' apartments were insulated. The common staircase and window reveals were also insulated in all six cases. Per apartment, 8–10 sensors were installed. They were installed at two different heights, one at the top (0.15 m from the ceiling) and the other at the center of the wall (1.25 m from the floor). In addition to interior insulation, mechanical ventilation with heat recovery was installed in all six apartments.

Indoor climate sensors were installed in the six reference apartments as well as in the six retrofitted apartments. The indoor climate was recorded from September 2014 to August 2015 and from March 2016 to June 2017, i.e., measurements were performed before and after the energy-saving measures were installed. To visually analyze the conditions at the interface and conduct mold testing, the insulation was removed in two of the apartments in summer 2017. In both occasions, the insulation was immediately re-established.

In this case, some in-situ mold testings were also implemented with the Mycometer test. The Mycometer test is a quantitative examination technique that demonstrates the degree of mold growth. The test is based on the identification and quantification of an enzyme present in the mycelium and spores of every kind of mold. The results can be divided into 3 categories:

- A: Mycometer value ≤ 25. The amount of mold is not excessive.
- B: 25 < Mycometer value ≤ 450. Mold contamination is above average. This may be as a result of older mold that has dried-out or the buildup of fungus spores in dust and dirt.
- C: Mycometer value > 450. The amount of mold is significantly higher than average. The result in this category, which is based on testings made in areas with high mold levels (bio-mass), shows rapid mold growth.

Fig. 3. Left: Top view of the building showing the covering of the neighboring property and the refurbished wall (yellow) [34] (Copyright Google Maps). Right: Drill core from original wall of case D. The outer part of the wall (on the left) is made of yellow brick and the inner part of lightweight clinker concrete (on the right). (For interpretation of the references to colour in this figure legend, the reader is referred to the web version of this article.)

2.3. Measurements of temperature and relative humidity

In each case, the sensors were installed at the interfaces either in preexisting joints or intentional holes created in the original wall. The information about the sensors is also found in [16,24,32,35–38] and are presented in Table 5.

2.4. Mold model

The Mold Index VTT 2.0 mold model [31,39] was applied on the measured temperature and relative humidity information to assess the potential mold risks. The Mold Index categorizes the amount of mold growth on a scale from 0 (no growth, no spore activation) to 6 (extremely heavy and tight growth, coverage about 100 %). For surfaces in contact with indoor air, safe limit is < 1, while a mold index < 3 is acceptable for locations without contact to indoor air [30,31,39].

The model index (M) is calculated based on equation (1) [40]. Factor t is time (h), T is temperature (^{o}C), RH is relative humidity (%), W is the timber species (0 = pine and 1 = spruce), and SQ is the surface quality (SQ = 0 for sawn surface, SQ = 1 for kiln-dried quality). Factors SQ and W were both set to zero for sawn surfaces and pine, respectively. The parameters k_1 (equation (2) and k_2 (equation (3) are correction coefficients for mold growth intensity and moderation of mold growth intensityas M approaches M_{max}, respectively. The factor $t_{M=1}$ is the time needed for the material to start the growth (mold index reaches level M = 1), and $t_{M=3}$ is the time needed for the material to reach level M = 3. The subscript "pine" refers to the value with the reference material pine. M_{max} (equation (4) is the maximum mold index achieved for each sensitivity class, and parameters A, B and C are constant related to the material sensitivity classes: Resistant, medium resistant, sensitive and very sensitive. RH_{crit} (%) is the limit relative humidity level to start the mold growth and is a function of temperature. It should be noted that, the Mold model is based on empirical formulas and the details and constant values for the Mold Index calculation can be found in [40].

In the current study, the "medium resistant" sensitivity class, which corresponds best to materials in the studied cases, was used as the default choice together with a relatively small decline of 0.25 for unfavorable growth conditions.

$$\frac{dM}{dt} = \frac{1}{7 \bullet e^{-0.68\ln(T) - 13.9\ln(RH) + 0.14W - 0.33SQ + 66.02}} \bullet k_1 k_2 \quad (1)$$

$$k_1 = \begin{cases} \dfrac{t_{M=1,pine}}{t_{M=1}}, M < 1 \\ 2 \bullet \dfrac{t_{M=3,pine} - t_{M=1,pine}}{t_{M=3} - t_{M=1}}, M > 1 \end{cases} \quad (2)$$

$$k_2 = max\begin{cases} 1 - e^{2.3(M - M_{Max})} \\ 0 \end{cases} \quad (3)$$

$$M_{max} = A + B \bullet \frac{RH_{crit} - RH}{RH_{crit} - 100} - C \bullet \left(\frac{RH_{crit} - RH}{RH_{crit} - 100}\right)^2 \quad (4)$$

To evaluate if there were any mold traces behind the insulation in case F, a visual assessment growth were conducted after removing the insulation in two apartments [41]. Several surface tests of mold growth were implemented in one of these apartments. Mycometer-Surface [42–44], which measures biomass but does not identify the kind of mold, was used for the measurements. If there is mold growth, the biomass amount will be considerably high. Thus, this type of test is a measure of the degree of growth on the surface. Five Mycometer tests were conducted. The sample locations were chosen based on where the risk of mold growth was assumed to be the highest. In addition some other mold tests were conducted: tape samples (microscopy) and impression samples.

3. Results

3.1. In situ measurements of temperature and relative humidity

3.1.1. Case M

Fig. 4 show the relative humidity and temperature measurements for case M for two time periods (2014–2018 before hydrophobization and 2020–2022 after hydrophobization) as hourly averages generated from minutely data. The external climate (T and RH) is running averages every two weeks for better readability. There is a gap of 2.5 years with no measurements. Prior to hydrophobization, sensors W2 and W4 (S oriented in the intersection) barely recorded relative humidity levels above 80 %, in contrast to W6 (SW oriented in the intersection), which peaked at 95 % during the second winter after insulation. The lowest humidity level at the beam ends was recorded in the post-hydrophobization period from July through September. The sensor at the interfaces with the highest relative humidity after hydrophobization was W4. Relative humidity is typically observed to be higher during the second measuring period compared to the first.

Except sensor W6, which had a 2–3 °C rise in winter temperature during the first three months after hydrophobization, all sensors' values for the temperature conditions in both periods are very similar and exhibit typical seasonal variation. In all cases, the temperature at the wall interface is higher than the beam ends, despite the thermal bridge. After hydrophobization, the interior temperature (sensor I1) gradually rises over the course of the year (by max. 4 °C). The external climate data (both T and RH) seem to follow the normal seasonal fluctuations. The humidity class of this case is calculated to be class 2 (dwellings with normal occupancy and ventilation).

3.1.2. Case B

Fig. 5 displays the results of the measurements for relative humidity and temperature in the intersection between the original wall and the insulation for the living room, bedroom, and spandrels of case B. The

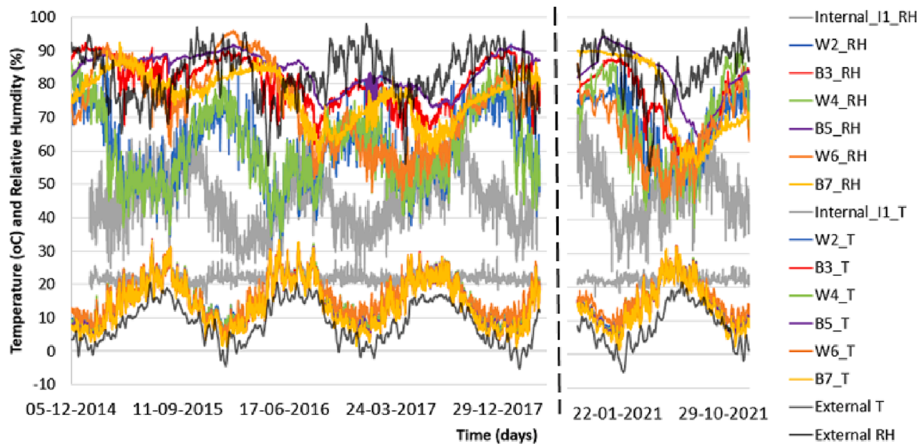

Fig. 4. Case M: Measured relative humidity and temperature in S (B3, W2) and SW (B5, B7, W4, W6) facade. Grey lines: indoor (sensor I1). Black lines: external weather conditions, obtained from DMI (Danish Meteorological Institute).

drying out period had various offsets, since the systems were not installed simultaneously [32]. Additionally, since the (yellow) sensor is mounted on the living room wall, these measurements should be regarded as interior climate measurements (Ref. = Indoor climate). Some measurements stopped earlier than others due to sensor malfunction. The external climate (T and RH) is running averages every two weeks for better readability. Winter 2019–2020 showed relative humidity up to 100 %. A1 sensors (north, hydrophobized) in the bedroom and living room showed the lowest relative humidity, whereas A3 sensors (north, non-hydrophobized) in the living room and bedroom consistently displayed the highest relative humidity. Relative humidity in all wall sensors generally drops after the first few months to 90 % the following winter.

Spandrels appear to be an exception, as the minimum relative humidity during warm months was approximately 70 % and the maximum was 100 % for the first nine months. Additionally, A2 sensors (south, hydrophobized) at the spandrels displayed significantly larger relative humidity fluctuations. The external climate data (both T and RH) seem

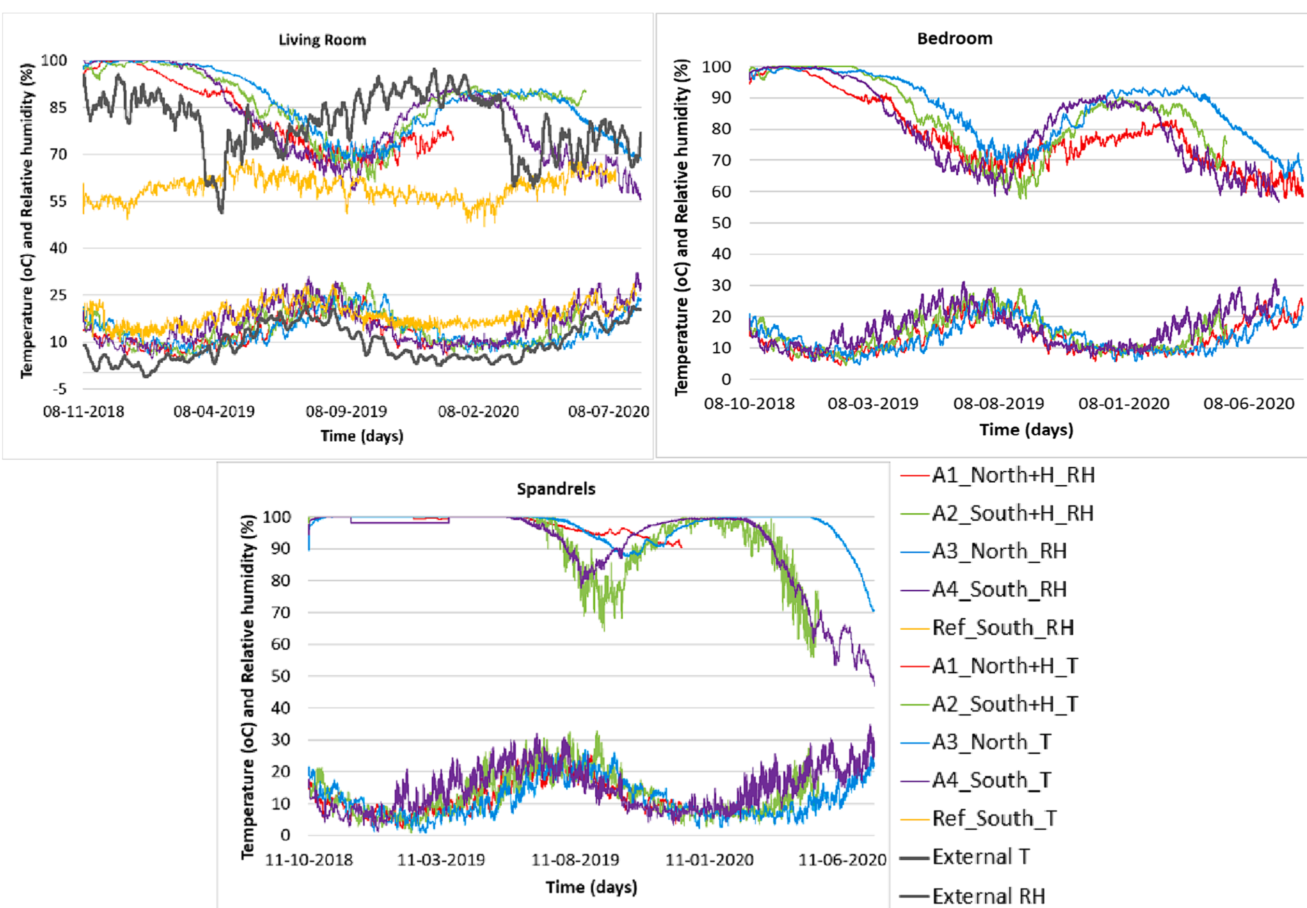

Fig. 5. Case B: Measurement data from a) living room + external climate (black lines), obtained from DMI (Danish Meteorological Institute), b) bedroom and c) spandrels for all four apartments.

to follow the normal seasonal fluctuations. The humidity class of this case is calculated to be class 2 (dwellings with normal occupancy and ventilation).

3.1.3. Case D

Fig. 6, Fig. 7 and Fig. 8 display the measurement results for case D. The measurements were interrupted for three months in 2017 because of sensor malfunction [24]. The wall is regarded as internal in the places where the gable is joined to the neighboring building; therefore, the sensors there roughly measured the indoor climate conditions (sensors 115, 114, 123, 125, 126 and 124), as presented in the graphs [24]. However, there were dedicated sensors (5503, 5524, 5507, 5506 and 5511) for measuring the indoor climate, but these sensors measured only for the period March 1016-July 2017 (see Fig. 6). The external climate (T and RH) is running averages every two weeks for better readability. The measurements in the interface between insulation and the existing wall were generally lower than 80 %. Measurements taken from the ground floor differed from those above; in the eastern bedroom, sensors 105 and 106 displayed higher values than those taken from the other measuring points. This increasing tendency started at winter 2019 and continued until 2022 when the measurements stopped. Relative humidity in the interface was above 90 % at this time, and one sensor (105) reached 100 % every winter before it decreased during spring times. These sensors' temperature measurements also indicated lower temperatures; in particular, sensor 106 showed a reduction in temperature up to 5 °C during the colder months. Additionally, relative humidity in the ground floor apartment seems to be higher from the beginning and keeps rising over the years while 1st and 2nd floor's RH stayed lower and only the last 1–2 years started to increase. The external climate data (both T and RH) seem to follow the normal seasonal fluctuations. The humidity class of this case is calculated to be class 2 (dwellings with normal occupancy and ventilation).

3.1.4. Case F

The hygrothermal measurements of case F are presented in Fig. 9, Fig. 10, Fig. 11, and Fig. 12. There are separate graphs for each floor and the staircase results. Some sensors stopped functioning after a short period, leaving 48 active sensors. In this case, there are no indoor climate sensors for measuring the indoor climate conditions. The insulation in the first-floor apartments was removed and re-established during summer 2017. As a result, measurements showed a sharp rise in relative humidity due to the wet adhesive mortar; thus the peaks in the graphs are disregarded and not further commented on. The external climate (T and RH) is running averages every two weeks for better readability.

On the ground floor, sensor 132 and 189, which displayed up to 85 % RH during the winter, are the sensors with the highest relative humidity values. On the 1st floor, sensors 133 and 172 displayed relative humidity values up to 85 % and slightly lower temperatures during winter 2021. However, for the remaining time, these measurements resembled the measurements of the other sensors. The seasonal variation on the 1st floor was similar to the ground floor. On the 2nd floor, sensors 177 and 178 diverge, reaching 80 % RH during winter periods. These sensors also measured lower temperatures. Sensors 171 showed up to 85 % RH in the first winters, and gradually increases over the next winters above 80 %. The deviation could be explained by the lower temperature measured in this sensor. Living room sensor 164 registers an expected seasonal range of 35–70 % RH and a minimum temperature of 15 °C. On the contrary, sensor 175 peaks at 85 %. However, during summer, the relative humidity falls below 70 %.

In the staircase (north facing), measurements have been made in the interface on the ground and 1st floor. The results revealed similar findings for the two floors. Relative humidity is shown to be higher in the ground floor sensor than the 1st floor, while temperature is the opposite. The external climate data (both T and RH) seem to follow the normal seasonal fluctuations. The humidity class of this case is calculated to be class 2 (offices, dwellings with normal occupancy and ventilation), with the staircase being class 1 (unoccupied buildings, storage of dry goods).

3.2. Mold index

The VTT Mold Index model [31,45,46] was used to evaluate the risk of mold growth in all cases. The Mold Index was calculated for all available sensors in all cases. For improved visual clarity, the y-axis in some cases goes up to 1 and not 6, which is the entire range of the mold index (0–6). Although this mold model was designed for free surfaces (surfaces in contact with the indoor air layer), it may also be applied to the interior of the structures. In our cases, for interfaces between the original wall and the internal insulation a Mold Index of less than 3 and not increasing over time is acceptable [39].

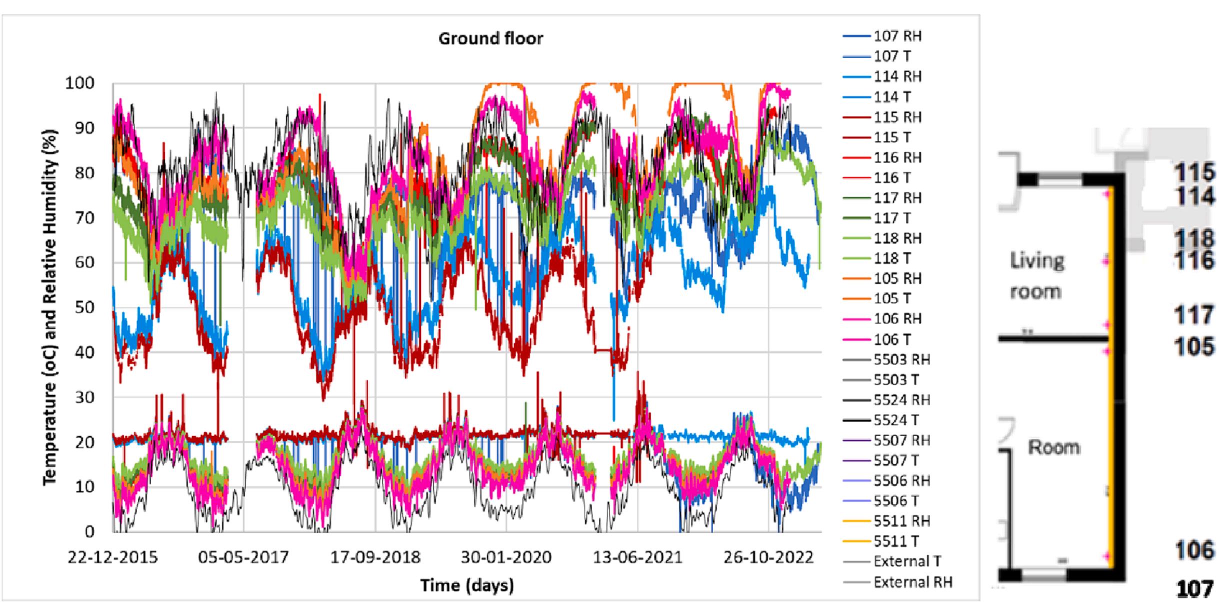

Fig. 6. Case D: Measurements of relative humidity and temperature from ground floor, Black lines: External climate, obtained from DMI (Danish Meteorological Institute).

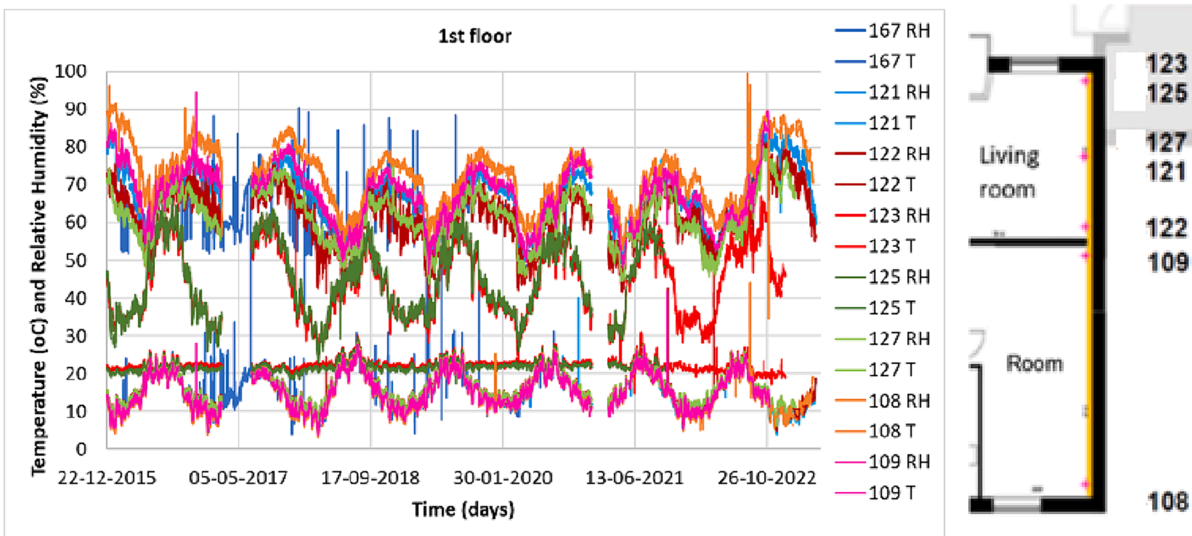

Fig. 7. Case D: Measurements of relative humidity and temperature from 1st floor.

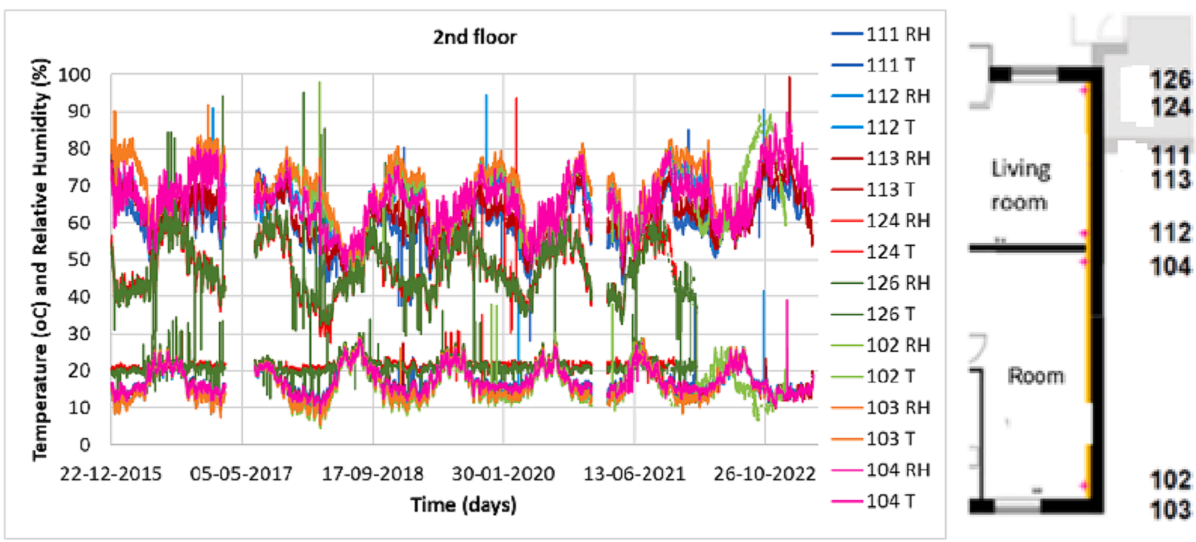

Fig. 8. Case D: Measurements of relative humidity and temperature from 2nd floor.

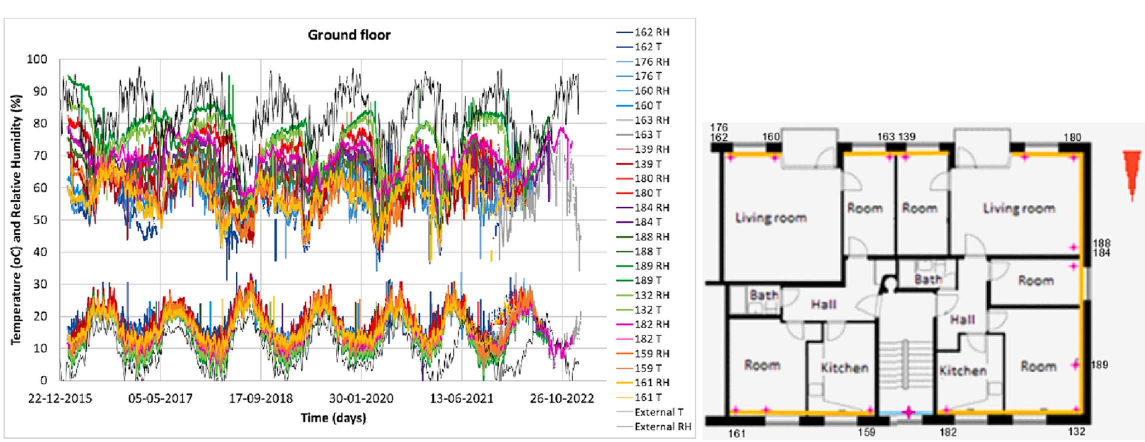

Fig. 9. Case F: Measurements of relative humidity and temperature from ground floor, Black lines: External climate, obtained from DMI (Danish Meteorological Institute).

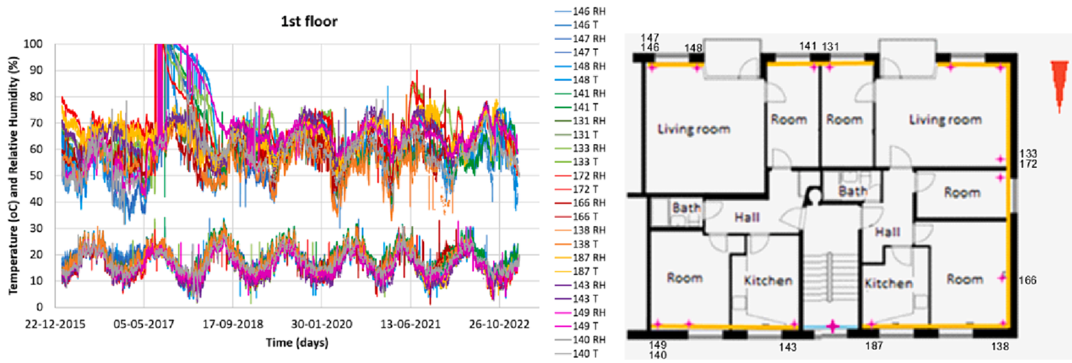

Fig. 10. Case F: Measurements of relative humidity and temperature from 1st floor.

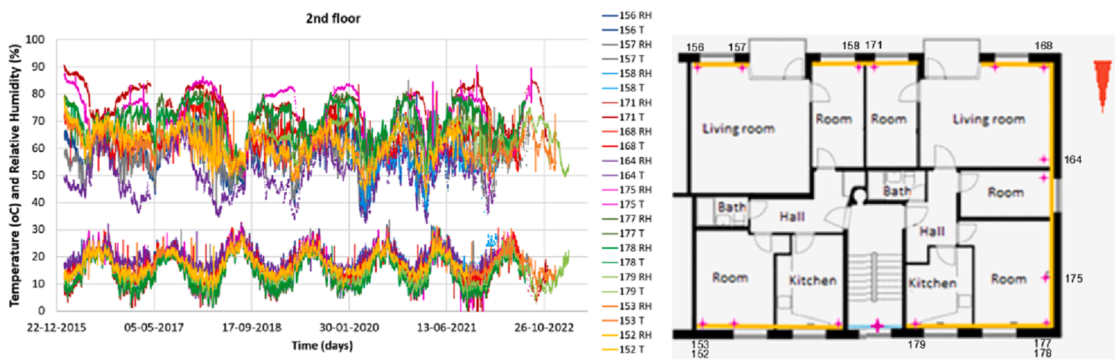

Fig. 11. Case F: Measurements of relative humidity and temperature from 2nd floor.

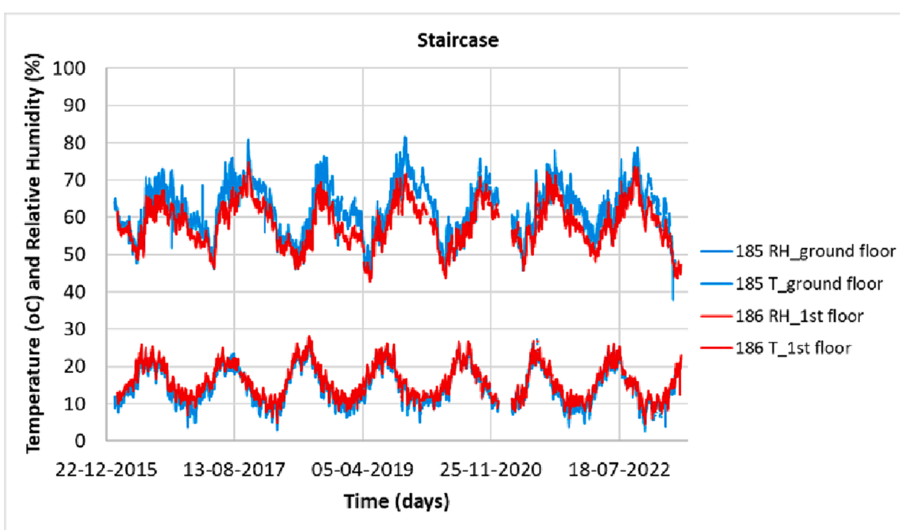

Fig. 12. Case F: Measurements of relative humidity and temperature from the staircase (north-facing) for ground and 1st floor.

3.2.1. Case M

Fig. 13 displays the risk of mold growth for Case M. Both measuring times—before and after hydrophobization—are shown in the graph. The mold growth index was practically zero and consistently below 1 in both periods. Only sensors B5 and W6 showed some mold growth initiation for the observed values prior to hydrophobization, although they never reached Mold Index 1. For sensors B5 and B7, the mold growth initiates during the post-hydrophobization phase. Furthermore, for all 3 sensors (W6, B5, and B7), the mold index, which had initially been somewhat above zero, quickly decreased to zero. In measurements made before hydrophobization, the Mold Index was found above zero both in the interface and the beam ends, however, after hydrophobization, this was only found at the beam ends.

3.2.2. Case B

Fig. 14 depicts the mold growth risk for case B. Except for the sensors at the spandrels, all sensors had a Mold Index of less than 1. All spandrels had a Mold Index higher than 2. Sensor A3_spandrels had the highest value of $M = 3$ between all spandrel sensors.

3.2.3. Case D

Fig. 15 presents the mold growth risk for case D. Winter 2019 was the first time when mold risk appeared specifically on the 1st floor. Two bedroom sensors, showed values above zero; sensor 105 displayed the

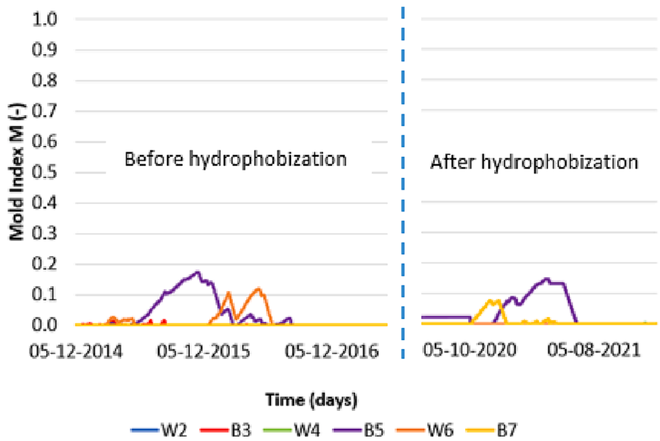

Fig. 13. Mold Index of case M, for interface and beam ends sensors as a function of time.

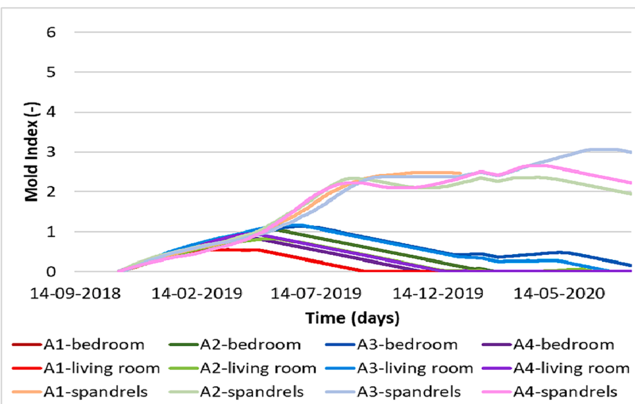

Fig. 14. Mold index of case B of all sensors as a function of time. Apartments: A1-N + H, A2-S + H, A3-N, A4-S.

maximum Mold Index of 3.5, while sensor 106 gave a value of less than 1. The assessed mold risk was practically equivalent to 0 for the other locations.

3.2.4. *Case F*

Fig. 16 shows the mold growth risk for case F. As a result of the re-installation of the insulation, there was initial built-in moisture, and several sensors indicated risk of mold growth with a maximum of almost 2, but it rapidly decreased. In the remaining time, sensors displayed lower mold index values with no risk of mold initiation.

In case F, there was also implemented some mycometer laboratory analyses for mold (Mycometer test).

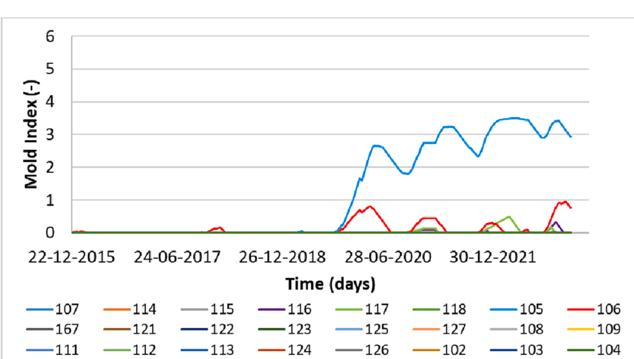

Fig. 15. Mold index of case D of all sensors as a function of time.

In general, the Mycometer test results have been at level A. A total of 17 Mycometer tests were taken. One of the tests was at B level, corresponding to value 34. A Mycometer test of level B usually indicates mold spores accumulation, but can also indicate mold growth. Even though the Mycometer number was 12 (level A), a pressure plate sample from the region revealed that more than 50 colony-forming units formed on the agar sample, indicating that there is a significant quantity of viable spores.

3.3. *Energy savings*

For cases F and D an energy savings investigation and calculation has been implemented. In case F, in addition to the internal insulation of the external walls, a balanced mechanical ventilation system with heat recovery was established as well. For case D, only the gable walls were refurbished. Table 7, compares the heat consumption for space heating in the experimental apartments with the consumption in the corresponding reference apartments for the heating period 2016–2017.

The heat consumption in case F, decreased by 24 % compared to the reference buildings, see Table 6, and the indoor temperature was 0.4 °C lower in the renovated apartments.

In case D, the heat consumption increased by 15 %. In these apartments the interior temperature was 1 °C warmer than the reference apartments. However, a comparison of the measurements of heat consumption between two periods, before and after the internal post insulation, was done (March 2015 and March 2016). The results show a reduction in the heat consumption of 0.42 MWh and almost the same indoor temperature of approx. 22°C. The saving corresponds to a reduction of 17 %. Also, the heating saving has been calculated and resulted in 0.43 MWh. There is therefore good agreement between measurements and calculations.

4. Discussion

This study focuses on the presumably most important parameters that influence the decision about the type of internal insulation that is suitable for older, Danish buildings, based on real-life measurements in a Danish setting. The considered factors are: hydrophobization, orientation, insulation system and indoor climate (with energy savings), and will be explained below.

4.1. *Hydrophobization*

In this study only cases M and B were hydrophobized and are the ones explained below.

The findings from the measurements in Case M demonstrated that applying hydrophobization after installing internal insulation with high water vapor diffusion resistance in an older building had both favorable and unfavorable impacts on the structure's hygrothermal response. A negative effect was that the relative humidity rose at the interface between the original wall and the insulation material compared to the time

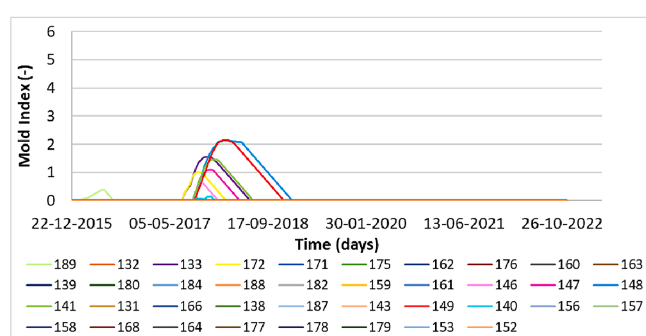

Fig. 16. Mold index of case F as a function of time.

Table 6
Measured heat consumption for space heating in the period April 2016 to March 2017 (1 year).

	Case F (Insulation and heat recovery) (6 apartments)	Case F (Reference) (6 apartments)	Case D (Gable insulation) (3 apartments)	Case D (Reference) (3 apartments)
Average internal temperature [°C]	22.2	22.6	21.4	20.4
Heat consumption [KWh]	31.189	41.052	16.210	14.080
Reduction [%]	24	–	−15	–

before hydrophobization. As hydrophobization prevents capillary suction, any water trapped behind the hydrophobized surface can only be evacuated to the outside through diffusion, a very slow process compared to capillary suction. Furthermore, diffusion resistance of the hydrophobized masonry is slightly higher than of an untreated masonry [10]. In addition, water can be trapped if the treatment had flaws that enabled water to enter. To allow the moisture to dry inwards, it is often advised to apply hydrophobization before the application of insulation. The wall needs longer time to reach moisture equilibrium if hydrophobization is applied after the insulation [1].

The influence of hydrophobization appears positive at the beam ends in Case M, where the measured relative humidity is lower at the wooden beam ends after hydrophobization than before. A possible explanation is that there is an uninsulated air gap just above the beam ends, so the drying inwards is not hampered by diffusion tight insulation material in this area. Since there was a big rain event at the end of September 2020 that might not have directly affected the wall (due to the scaffold) before the application of hydrophobization, but undoubtedly raised the external relative humidity, thus the initial increase for a short time after treatment was anticipated. However, it is unclear if the lower humidity levels at the beam ends resulted from hydrophobization's effectiveness, diffusion open interior surface (or combination of these) or the warmer winters, but the relative humidity was generally lower than the time before hydrophobization. It appears that hydrophobization has the least impact on the interface temperature.

None of the investigated locations in either period achieved Mold Index 1. This might imply that the site's interior insulation installation and hydrophobization processes were successfully carried out, resulting in a vapor-tight system and a well-hydrophobized façade. Another explanation could be that the first winter following the treatment was comparatively mild; the freshly placed hydrophobization was not subjected to adverse weather.

In Case B, the built-in moisture was most probably dried out throughout the first winter season (2018–2019). The moisture content was significantly lower in the following winter. In the last 10 months of 2020, hydrophobization appeared to have a positive impact on the northern gable while having little or negative impact on the southern gable, which got the most WDR. This is unexpected because according to e.g. Jensen [25], the effect of hydrophobization is most noticeable in walls with a lot of WDR. That, however, was based on measurements in a lab-like facility (brick wall section cut into a container with a controlled indoor environment and at ground level), which, compared to this study, is much more favorable for a successful hydrophobization.

The measurements in case B show:

- Hydrophobization in walls with a north orientation (reduced WDR) appears to be a successful combination (A1-lowest RH) with a diffusion open internal insulation.
- The northern wall without hydrophobization, A3, always had the highest RH. In comparison, in the south-oriented walls, the ability of the sun to dry outwards the moisture helped keeping the humidity levels lower.

In both cases, the Mold Index does not exceed the value of 1, except in the spandrels of case B where a Mold index of 3 is achieved. However, no obvious effect regarding the different orientations or different cases (with and without hydrophobization) was noticed.

4.2. Orientation

In all cases, except case M, a variety of apartments were tested on different floors and orientations. Case M has mainly S (and SW) orientation so no obvious differences could be seen regarding direction.

The measurements in case B show that:

- South-oriented walls may have the highest relative humidity most of the time (A2 and A4), due to the strong WDR in that direction.
- Floor levels appear to be important in respect to assumed run off which is expected to increase for lower floors. A2 (hydrophobization-2nd floor) experiences more run offs than A4 (no hydrophobization-5th floor), where the WDR is higher, and generally, the relative humidity of A2 is higher than A4, so WDR appears to be less significant than the run off.

In case F, although sensor 171 on the 2nd floor's southern façade varied from the norm by showing a slightly higher relative humidity and lower temperature than the normal seasonal fluctuation, the risk of mold growth is minuscule. Sensors 177 and 178 on the 2nd floor diverge, reaching 80 % RH in the winter, resulting in a very low risk of mold when combined with low temperatures. Sensor 175, on the other hand, peaks at 85 %. However, the relative humidity drops below 70 % in the summer. The measurements in the west-facing gable generally reveal acceptable conditions; $<$75 % RH and $<$ 1.5 max Mold Index. Conclusively, the orientation does not seem to make a difference considering risk of mold growth.

4.3. Insulation system

Regarding the insulation systems, several insulation materials as well as thicknesses were investigated. In this section the most important findings are discussed.

Case B, is the only case where there are measurements from the spandrels, where the wall thickness is smaller. In that case, the spandrels' exceptionally high relative humidity may be caused by a combination of the thick insulation, which decreases the wall's temperature, and the thinner wall, which increases the risk of water penetration. Thus, the moisture risk in the spandrels is higher than in the regular walls. The results demonstrate that the mold risk is relatively high in the spandrels, and, therefore, they cannot be characterized as moisture-safe.

In case F, despite the relatively high relative humidity measured, there is no increased risk for mold growth. None of the measurements achieved mold index higher than 2. Furthermore, the two locations with the highest mold index, reached these values only because of the built-in moisture (re-establishment of internal insulation). The result of the mold testing when the insulation was removed in the 2nd floor apartment confirmed that after 2 years there was none or very little mold at the intersection (low mycometer values). Thus, the mold risk calculation and the mold testing agree and they both show that there is no risk of mold growth in that case.

A similarity between the four cases is that none of them are expected to face the severe risk of mold growth, except for the spandrels, where the masonry is thinner and the insulation thicker. The higher calculated

Table 7
Summary of the four cases.

Description						Results			
Case	Orientation	Insulation thickness (mm)	R-value (m^2K/W)	Hydrophobization	System	Indoor climate	RH (%) (winter)	Mold (max) (−)	Outcome
M	S	60	3	−	Tight	~ 2	75–85	0	+
	SE			−			70–95	0.1	
	S			+			75–90	0	
	SE			+			75–80	0	
M (beam ends)	S			−			80–90	0.18	
	SE			−			80–90	0	
	S			+			80–95	0.15	
	SE			+			80–90	0.07	
B	N	100	2.38	−	Open	~ 2	90	1	+
	N			+			80	0.7	
	S			−			90	1	
	S			+			90	1	
B (spandrels)	N	220	5.24	−			100	>2	(−)
	N			+			100	2.5	
	S			−			100	2.5	
	S			+			100	2.5	
D	N	80	1.9	−	Open	~ 2	70–90*	0*	(+) but might be critical in ground floor
F	N	50 (façade)	1.51	−	Tight	~ 2	70–85	2**	+
	S			−		~ 2	65–80	2**	
	W	80 (gable)	2.42	−		~ 2	70–85	1.3	
F (staircase)	N	50	1	−	Open	~ 1	70–80	0	

*Ground floor 80–100 % RH, Mold index > 3.
**Re-establishment of new insulation

mold growth risk in regular walls appears right after applying insulation (build-in moisture) where the pH value is high, and mold growth can therefore be assumed inhibited. Another similarity is that the relative humidity is generally not above 90–95 %. Moreover, the temperatures in all cases follow normal seasonal fluctuations.

Cases D and B have the same insulation material but in different thicknesses (80 and 100 mm). The calculated mold index in both cases remains in low levels (max 1), except the spandrels in case B (max 2.5) where the wall is thinner, and the insulation is thicker. Finally, all cases have the same thickness of original wall (360 mm). The U-value of the existed wall is approximately 1.67 W/m^2K. Maybe an improvement of the U-value may be the key: if it is too high (like in the spandrels) the risk of the interface being at a too cold place is too high (like the vapor barrier). On the other hand, if the wall is too thin it has a higher risk of becoming wet at the interface due to capillary suction, defects etc. Furthermore, the insulation thicknesses differ from case to case and range from 60-100 mm. The external walls in cases M and B are solid masonry while cases D and F, which belong in the same building complex, have mixed masonry (half-brick, half-lightweight clinker concrete). This results in slightly different wall properties even if the total original wall thickness is the same (360 mm). However, the different materials of the original walls do not seem to have any influence on the results. Finally, comparing cases B and D (both diffusion open) it can be seen that the mold risk is minimum to non-existent and the systems seems to perform efficiently. Regarding cases M and F (both diffusion tight), it can be seen that the outcome is also positive, but the mold growth risk is higher in these cases and there are certain locations (ground floor next to the kitchen) where the conditions are even more critical.

4.4. Indoor climate and energy savings

While the indoor climate was monitored in all cases, the energy savings were measured only for cases D and F. The energy savings were measured with sensors measuring the heat consumption [47].

In Case D, the main moisture load is assumed to be from indoor air. The increased relative humidity behind the insulation in one of the rooms on the ground floor indicated that there must have been a high humidity load, and it is limited how much moisture this capillary active insulation material can carry back to the interior climate. The indoor moisture content in all floors had a moisture excess corresponding to humidity class 2. However, these estimations have a high degree of uncertainty as the indoor climate measurements that were used were the ones from the part of the building which is adjacent to the neighboring one. It must also be noted that the indoor climate measurements in case D and F only took place during the first year after the installation of the insulation and do not cover the last time period with monitored high moisture levels behind insulation.

Except for the room on the ground floor, the mold model predicted no mold growth risk behind the insulation. This one sensor that recorded 100 % relative humidity during the most recent winter season reached a Mold Index of 3.5 before decreasing along with the relative humidity. This high moisture level can only be explained by a high interior moisture load during the last period of the measurements, when residents' behavior might have changed, e.g. very low ventilation rates or/and high moisture production.

In Case F, the relative humidity at sensor 132 and 189 (ground floor) peaked during winter at 85 % RH, so they deviate from the other data. Additionally, this sensor registers lower temperatures, which results in higher relative humidity. The bedroom's corner, which is next to the gable, registers relatively low temperature. However, the results demonstrate that the conditions at the interface are influenced by user behavior and the interior climate, as the sensor on the 1st floor in the same place registers higher temperature and lower relative humidity.

The staircase is an area that none stays for longer times, thus the moisture load there is likely to be minimal. The staircase sensor on the ground floor registers somewhat higher relative humidity and slightly lower temperatures. However, that sensor was closer to the front door, which often opens during the day, fact that explains this.

The highest relative humidity levels combined with lower temperatures are generally found in the gables, which are insulated with thicker insulation than the facades. Before refurbishment Case F apartments were classified as moisture load class 3. However, the moisture class was reduced to 2 due to the mechanical ventilation that also was established.

The amount of data on energy consumption is the same in the two cases (cases D and F). However, data from more apartments makes the result more valid for case F (3 and 6 apartments, respectively). Also, according to residents' interviews, it is likely that differences in habits (especially residential density, cooking, use of lighting) results in differences in heating usage.

In case D, the heat consumption in the renovated apartments was higher than in the reference apartments, this was surprising, but the indoor temperature was 1 °C higher in the renovated apartments, indicating very different user behavior. Consequently, the heat consumption in the renovated apartments for March 2015 (prior to insulation installation) was compared with March 2016 (after renovation) to address these uncertainties. The temperatures outside and indoors were similar in these two months. This comparison showed a reduction in energy consumption by 17 % which was also the prediction which was done with calculations. The residents have experienced an improvement in the indoor climate in the form of reduced drafts from the outer walls, while the ventilation pattern has remained unchanged. The average temperature in the indoor climate has not changed significantly because of the implemented energy savings.

In case F, the indoor climate measurements and the moisture content calculation showed that 22 % can be saved on space heating by insulating all external walls internally and establishing balanced mechanical ventilation. Unfortunately, the ventilation system results in higher power usage. This energy usage is equal to the savings from heat recovery (1.0 MWh/year). In that case, there was a relatively low air exchange initially, which is primarily why all the savings from heat recovery were used for ventilation rather than because power consumption was not considered when designing the ventilation system. The air exchange was doubled when the ventilation system was installed. After installing the ventilation system, the infiltration—which is not covered by heat recovery—is up to around 30 % of the air change.

According to the hypothesis of this project, orientation, indoor climate, hydrophobization and insulation thickness and type and the wall thickness play a role in the outcome of the measurements. This study showed that all these parameters seem to be decisive, thus one should be cautious with comparing the different cases.

Table 7 is a summary of the systems' characteristics, winter relative humidity, mold growth index as well as the outcome that appear in the four cases which are being studied.

4.5. Limitations

There are some limitations that need to be considered in the current study of the four cases.

1. Since the sensors have not been re-calibrated during the measurement period, the data may have an increasing error rate.
2. The results do not always concern watertight walls. There may be either differences in the quality of the work between facades that have been repointed or the facades that have been visually accessed cannot be assumed as completely watertight.
3. The effectiveness of the hydrophobization treatment is affected by parameters like the local climate and the hygrothermal properties of the building materials (brick and mortar) [14].
4. Given that the system is being examined in real-life conditions, it is likely to have flaws because of human application errors.

All the aforementioned limitations should be considered since they influence the results of the real-life measurements. Meaning that these are only a few cases, and therefore just examples of outcomes that may describe a trend. But there will be a variety of outcomes for different settings. Special attention should always be paid to each construction's special features and details.

5. Conclusion

The outcome of the measurements from the four cases demonstrates an acceptable moisture-safety of the chosen insulation systems and typical thicknesses. During the time of measurement, there was no general indication of wetting in the constructions. Most sensors present values that are below the threshold for mold growth. Furthermore, it may be anticipated that the adhesive mortar's initial high pH will inhibit any potential mold growth during the initial period of high moisture load. More specifically:

- In terms of hydrophobization, it is showed that there is a risk of WDR absorption if the hydrophobization is applied after the internal insulation (case M). This may result in moisture trapped between internal insulation and the applied hydrophobization and exhibits lower drying rates. This fact is even more severe in the case of vapor tight insulation system, as in case M. Also, the studied cases show, rather surprisingly, that hydrophobization works better in the north direction where less WDR and sun radiation exists (case B).
- Regarding orientation, it was noticed that the direction of the façade and floor level plays a role in the moisture levels. The orientation is of less importance than the floor level; the lower the floor the higher the risk, since it is likely that the runoff volume is more significant than direct WDR (case B).
- When using diffusion-open solutions, it is crucial that the indoor climate is not too humid because this increases the risk of high moisture levels in the construction during the colder months. The elevated humidity behind diffusion open insulation in the single room in case D illustrates this clearly. Also, case D showed that even though the maximum Mold Index was calculated to 3.5 which normally is not on the safe side for the inside of structures, it only appears in one specific location, presumably due to higher moisture loads and/or lower ventilation rates than expected. Apart from that, there is no obvious risk of mold growth.
- In the cases with humidity class 2 or lower there is no general risk of mold growth, especially if the high indoor moisture loads are regulated by mechanical ventilation system (case F).
- In terms of energy savings, internal insulation reduces energy consumption for space heating as expected, unless these savings are transferred to higher indoor temperature.

Overall, there are no apparent distinctions in the performance of the various systems. No system stands out in comparison to the others. All systems can display acceptable moisture-related conditions. However, the variations in the apartments' interior climates, residents, orientations, and floor levels pointed out that indoor climate and residents' behavior plays a vital role in the hygrothermal performance of the system. In addition, the results showed that orientation has less effect on the moisture levels and hydrophobization performs better in the north orientation where there is less sun and WDR. For future cases to follow the methodology and practices given in the current study, the hygrothermal and system parameters should be comparable to those examined here for being robust and moisture safe.

CRediT authorship contribution statement

Panagiota Pagoni: Writing – review & editing, Writing – original draft, Validation, Software, Investigation, Formal analysis. **Eva B. Møller:** Writing – review & editing, Validation, Supervision, Methodology, Investigation, Conceptualization. **Ruut H. Peuhkuri:** Writing – review & editing, Validation, Supervision, Resources, Investigation, Funding acquisition.

Declaration of competing interest

The authors declare the following financial interests/personal relationships which may be considered as potential competing interests: Ruut Hannele Peuhkuri reports financial support was provided by Realdania. Ruut Hannele Peuhkuri reports financial support was provided by Grundejernes Investerings Fond. Ruut Hannele Peuhkuri reports financial support was provided by Landsbyggefonden. If there are other authors, they declare that they have no known competing financial interests or personal relationships that could have appeared to influence the work reported in this paper.

Data availability

The supplementary data of the research will be shared in DTU data management website.

Acknowledgments

Case M is a part of the project “Moisture safe energy renovations” funded by Grundejernes Investerings Fond, Landsbyggefonden (The Landowners’ Investment Foundation and The National Building Foundation) and Realdania. The data used for this study are a continuation of measurements performed for the EUDP project 2013-II: “Energy efficient comfort in older apartment blocks”. Case M has been provided by Arup & Hvidt. Cases D and F were initiated in collaboration with the Municipality of Copenhagen, and 3B (KAB) and were financed by funds from Copenhagen Municipality and BUILD. Furthermore, Niels Peter Kloch (BMT Instruments ApS) is acknowledged for commissioning the measurement equipment, and Technological Institute for conducting some of the mold tests. Moreover, Realdania and Xella are acknowledged for financial support, materials, and craftsmanship in case B.

References

[1] S. Hansen, Peuhkuri, Hygrothermal performance of hydrophobized and internally insulated masonry walls - Simulating the impact of hydrophobization based on experimental results, Building and Environment, vol. 187, no. September 2020, p. 107410, 2021, doi: 10.1016/j.buildenv.2020.107410.
[2] B. Hansen, Peuhkuri, Hansen, Performance of hydrophobized historic solid masonry – experimental approach”, Constr. Build. Mater. 188 (2018) 695–708, https://doi.org/10.1016/j.conbuildmat.2018.08.145.
[3] P. Pagoni, E.B. Møller, T.K. Hansen, Hygrothermal measurements in internally insulated solid masonry wall before and after hydrophobization, in AIP Conference Proceedings, 2023, vol. 2918, no. 1, doi: 10.1063/5.0171209.
[4] P. Pagoni, E.B. Møller, T.K. Hansen, Internal insulation of masonry with and without hydrophobization in inhabited dwellings, in ASHRAE Buildings XV Conference, 2022, p. 726.
[5] A. Blumberga et al., RIBuild: State of the art on historic building insulation materials and retrofit strategies, p. 87, 2016, [Online]. Available: https://www.ribuild.eu/s/RIBuild_D12_10.pdf [Accessed: 15-September-2023].
[6] N.F. Jensen, Robust solutions for internal retrofitting solid masonry walls in historic buildings with regards to hygrothermal performance, p. 287, Ph.D Thesis, Technical University of Denamrk, 2021, [Online]. Available: https://orbit.dtu.dk/files/270624466/Phd_thesis_Nickolaj.pdf.
[7] P. Johansson et al., RIBuild: robust internal thermal insulation of historic buildings - threshold values for failure, linked to types of building structures and failure modes, 2019. [Online] Available: https://www.ribuild.eu/s/RIBuild_D22_v10_1.pdf [Accessed: 15-September-2023].
[8] B. Jensen, Rode, Møller, Hygrothermal assessment of four insulation systems for interior retrofitting of solid masonry walls through calibrated numerical simulations, Build. Environ. 180 (2020), https://doi.org/10.1016/j.buildenv.2020.107031.
[9] E. Brandt et al, Fugt i bygninger- Bygningsdele, SBi-anvisning 279, BUILD, Aalborg Universitet. 2022.
[10] H. Soulios, Feng, Janssen, Hygric behavior of hydrophobized brick and mortar samples, Build. Environ. vol. 176, no. March (2020) 106843, https://doi.org/10.1016/j.buildenv.2020.106843.
[11] V. Soulios, Hygrothermal performance of hydrophobized brick and mortar - energy renovation through internal insulation - can hydrophobization improve the moisture safety?, Ph.D Thesis, Aalborg University, 2021.
[12] T.K. Hansen, R.H. Peuhkuri, Slutrapport – Vurdering af fugtforhold bag indvendig efterisolering efter flere års målinger Demonstrationsprojekt om indvendig efterisolering i 3B’s afdelinger Druehaven 5 og Folehaven 75, Institut for Byggeri, By og Miljø (BUILD), Aalborg Universitet. BUILD Rapport Bind 2023 Nr. 19, 2023.
[13] E.J. De Place Hansen, E.B. Møller, M. Ørsager, Guidelines for internal insulation of historic buildings, E3S Web Conf. 172 (2020), https://doi.org/10.1051/e3sconf/202017201004.
[14] E.B. Møller, RIBuild: Report on the material properties, Eur. Univ. Inst., no. 2, pp. 2–5, 2018, [Online]. Available: https://www.ribuild.eu/s/RIBuild_D21_v10.pdf. [Accessed: 15-September-2023].
[15] A. Blumberga et al., RIBuild: Report on historical building types and combinations of structural solutions, Eur. Univ. Inst., no. 2, p. 149, 2017, [Online]. Available: http://hdl.handle.net/10603/223973%0Ahttps://shodhganga.inflibnet.ac.in/handle/10603/223973. [Accessed: 15-September-2023].
[16] B. Hansen, Peuhkuri, Harrestrup, Long term in situ measurements of hygrothermal conditions at critical points in four cases of internally insulated historic solid masonry walls, Energ. Buildings 172 (2018) 235–248, https://doi.org/10.1016/j.enbuild.2018.05.001.
[17] T. Odgaard, S.P. Bjarløv, C. Rode, Interior insulation – experimental investigation of hygrothermal conditions and damage evaluation of solid masonry façades in a listed building, Build. Environ. 129 (2018) 1–14, https://doi.org/10.1016/j.buildenv.2017.11.015.
[18] B. Hansen, Peuhkuri, The effects of wind-driven rain on the hygrothermal conditions behind wooden beam ends and at the interfaces between internal insulation and existing solid masonry, Energ. Buildings 196 (2019) 255–268, https://doi.org/10.1016/j.enbuild.2019.05.020.
[19] N.F. Jensen, S.P. Bjarløv, C. Rode, T.R. Odgaard, Hygrothermal assessment of internally insulated solid masonry walls fitted with exterior hydrophobization and deliberate thermal bridge, Ce/papers 2 (4) (2018) 79–87, https://doi.org/10.1002/cepa.868.
[20] M. Harrestrup, S. Svendsen, Internal insulation applied in heritage multi-storey buildings with wooden beams embedded in solid masonry brick façades, Build. Environ. 99 (2016) 59–72, https://doi.org/10.1016/j.buildenv.2016.01.019.
[21] J. Toman, A. Vimmrová, R. Černý, Long-term on-site assessment of hygrothermal performance of interior thermal insulation system without water vapour barrier, Energ. Buildings 41 (1) (2009) 51–55, https://doi.org/10.1016/j.enbuild.2008.07.007.
[22] R. Walker, S. Pavía, Thermal performance of a selection of insulation materials suitable for historic buildings, Build. Environ. 94 (P1) (Dec. 2015) 155–165, https://doi.org/10.1016/J.BUILDENV.2015.07.033.
[23] P. Klõšeiko, E. Arumägi, T. Kalamees, Hygrothermal performance of internally insulated brick wall in cold climate: field measurement and model calibration, Proc. 2nd CESBP, no. Scheffler, 2013, [Online]. Available: https://www.etis.ee/ShowFile.aspx?FileVID=70890.
[24] Hansen, Peuhkuri, Demonstrationsprojekt om indvendig efterisolering i 3b’s afdelinger druehaven 5 og folehaven 75. Build 2020. Slutrapport. (Delrapport 3), 2020.
[25] O. Jensen, B. Andersen, R. Møller, Hygrothermal assessment of diffusion open insulation systems for interior retrofitting of solid masonry walls, Build. Environ. 182 (2020), https://doi.org/10.1016/j.buildenv.2020.107011.
[26] R. Jensen, B. Andersen, Møller, Internal insulation of solid masonry walls - Field experiment with Phenolic foam and lime-cork based insulating plaster, E3S Web Conf. 172 (2020) 1–8, https://doi.org/10.1051/e3sconf/202017201003.
[27] “WHO guidelines for indoor air quality : dampness and mould.” 2009, [Online]. Available: https://www.who.int/publications/i/item/9789289041683.
[28] T. Kvist Hansen, N. Feldt Jensen, E. Møller, E. Jan De Place Hansen, R. Peuhkuri, Monitored conditions in wooden wall plates in relation to mold and wood decaying fungi, E3S Web Conf. 172 (2020) 1–8, https://doi.org/10.1051/e3sconf/202017220004.
[29] B. Jensen, R. Andersen, Møller, Laboratory-based investigation of the materials’ water activity and pH relative to fungal growth in internally insulated solid masonry walls”, Indoor Air 31 (4) (2021) 1252–1266, https://doi.org/10.1111/ina.12796.
[30] H. Viitanen, M. Krus, T. Ojanen, V. Eitner, D. Zirkelbach, Mold risk classification based on comparative evaluation of two established growth models, Energy Procedia 78 (Nov. 2015) 1425–1430, https://doi.org/10.1016/J.EGYPRO.2015.11.165.
[31] Hukka, Viitanen, A mathematical model of mould growth on wooden material, Wood Sci. Technol. 33 (6) (1999) 475–485, https://doi.org/10.1007/s002260050131.
[32] Janssen et al., RIBuild: Impact of water repellent agents on hygric properties of porous building materials, p. 159, 2020, [Online]. Available: https://eur-lex.europa.eu/legal-content/PT/TXT/PDF/?uri=CELEX:32016R0679&from=PT%0Ahttp://eur-lex.europa.eu/LexUriServ/LexUriServ.do?uri=CELEX:52012PC0011:pt:NOT.
[33] ISO - International Standard Organization, “ISO 13788:2012 Hygrothermal performance of building components and building elements - Internal surface temperature to avoid critical surface humidity and interstitial condensation - Calculation methods,” Build. Stand. Inst., 2012.
[34] E.B. Møller, Demonstrationsprojekt om indvendig efterisolering i 3B ’ s afdelinger Druehaven 5 og Folehaven 75: Vurdering af forhold mht . skimmelrisiko et år efter opsætning (delrapport 1), no. delrapport 1, pp. 1–23, 2016.

[35] BMT instruments Hygro-I T/RF. http://bmtinstruments.dk/shop/hygro-i-t-rf-283p.html.
[36] "Lascar electronics." https://www.lascarelectronics.com/?gclid=Cj0KCQiA9.
[37] "Onset 2020b. HOBO U12-012 Data Logger data sheet." https://www.onsetcomp.com/datasheet/U12-012.
[38] "Rotronic 2019." https://www.rotronic.com/en-ch/hc2a-s.html.
[39] T. Ojanen, K. Lähdesmäki, J. Vinha, K. Salminen, Classification of material sensitivity-New approach for mould growth modeling Nordic Symposium of Building Physics, vol. 2, 2011, [Online]. Available: http://www.tut.fi/nsb2011/sites/www.tut.fi.nsb2011/files/b10_02_tuomo_ojanen_vtt_nordic_9th_classification_mould_growth_final2.pdf.
[40] T. Ojanen, H. Viitanen, R. Peuhkuri, J. Vinha, K. Salminen, Mold growth modeling of building structures using sensotivity classes of materials, Proceedings of 11th International Conference on Thermal Performance of the Exterior Envelopes of Whole Buildings, Buildings XI, Clearwater, USA, 2010.
[41] E.B. Møller, S.B. Jørgensen, Demonstrationsprojekt om indvendig efterisolering i 3B's afdelinger Druehaven 5 og Folehaven 75 Vurdering af forhold mht. skimmelrisiko to år efter opsætning (delrapport 2), 2018.
[42] M. Reeslev, M. Miller, The MycoMeter-test: a new rapid method for detection and quantification of mold in buildings, in Proceedings of Healthy Buildings, 2000, p. vol. 1, pp. 589 – 590.
[43] MycoMeter, The MycoMeter-test: a guide for the detection and quantification of molds in buildings, in The MycoMeter Handbook, Copenhagen, Denmark, 2002, pp. 1 – 39.
[44] "Mycometer Surface Fungi." [Online]. Available: www.mycometer.com.
[45] K. Viitanen, E. Ojanen, Zirkelbach, Mold risk classification based on comparative evaluation of two established, Growth Models 78 (2015) 1425–1430, https://doi.org/10.1016/j.egypro.2015.11.165.
[46] T. Ojanen, R. Peuhkuri, V. Lähdesmäki, V. Salminen, Classification of material sensitivity–new approach for mould growth modeling,… Nord. Symp. …, vol. 2, no. 9, pp. 867–874, 2011, [Online]. Available: http://webhotel2.tut.fi/nsb2011/sites/webhotel2.tut.fi.nsb2011/files/b10_02_tuomo_ojanen_vtt_nordic_9th_classification_mould_growth_final2.pdf.
[47] "Energy savings sensor Kamstrup, Multical 602." https://www.kamstrup.com/da-dk/varmeloesninger/intelligente-varmemaalere/discontinued-products/multical-602.